Atmospheric
Chemistry
and Physics
Discussions

1 **Measurement report: PM$_{2.5}$-bound nitrated aromatic compounds in Xi'an,**

2 **Northwest China: Seasonal variations and contributions to optical properties of**

3 **brown carbon**

4

5 Wei Yuan[1,6], Ru-Jin Huang[1,2], Lu Yang[1], Ting Wang[1,6], Jing Duan[1,6], Jie Guo[1], Haiyan Ni[1,7],

6 Yang Chen[3], Qi Chen[4], Yongjie Li[5], Ulrike Dusek[7], Colin O'Dowd[8], Thorsten Hoffmann[9]

7

8 [1]State Key Laboratory of Loess and Quaternary Geology, Center for Excellence in Quaternary

9 Science and Global Change, Key Laboratory of Aerosol Chemistry & Physics, Institute of Earth

10 Environment, Chinese Academy of Sciences, Xi'an 710061, China

11 [2]Institute of Global Environmental Change, Xi'an Jiaotong University, Xi'an 710049, China

12 [3]Chongqing Institute of Green and Intelligent Technology, Chinese Academy of Sciences,

13 Chongqing 400714, China

14 [4]State Key Joint Laboratory of Environmental Simulation and Pollution Control, College of

15 Environmental Sciences and Engineering, Peking University, Beijing 100871, China

16 [5]Department of Civil and Environmental Engineering, Faculty of Science and Technology,

17 University of Macau, Taipa, Macau SAR 999078, China

18 [6]University of Chinese Academy of Sciences, Beijing 100049, China

19 [7]Centre for Isotope Research (CIO), Energy and Sustainability Research Institute Groningen

20 (ESRIG), University of Groningen, 9747 AG, The Netherlands

21 [8]School of Physics and Centre for Climate and Air Pollution Studies, Ryan Institute, National

22 University of Ireland Galway, University Road, Galway H91CF50, Ireland

23 [9]Institute of Inorganic and Analytical Chemistry, Johannes Gutenberg University Mainz,

24 Duesbergweg 10−14, 55128 Mainz, Germany

25 *Correspondence to*: Ru-Jin Huang (rujin.huang@ieecas.cn)

26

27

28   **Abstract**

29   Nitrated aromatic compounds (NACs) are a group of key chromophores for brown carbon

30   aerosol (light absorbing organic carbon, i.e., BrC), which affects radiative forcing. The

31   chemical composition and sources of NACs and their contributions to BrC absorption, however,

32   are still not well understood. In this study, $PM_{2.5}$-bound NACs in Xi'an, Northwest China, were

33   investigated for 112 daily $PM_{2.5}$ filter samples from 2015 to 2016. Both the total concentrations

34   and contributions from individual species of NACs show distinct seasonal variations. The

35   seasonally averaged concentrations of NACs are 2.1 (spring), 1.1 (summer), 12.9 (fall), and

36   56.3 ng m^{-3} (winter). Thereinto, 4-nitrophenol is the major NAC component in spring (58%).

37   The concentrations of 5-nitrosalicylic acid and 4-nitrophenol dominate in summer (70%), and

38   the concentrations of 4-nitrocatechol and 4-nitrophenol dominate in fall (58%) and winter

39   (55%). The NAC species show different seasonal patterns in concentrations, indicating

40   differences in emissions and formation pathways. Source apportionment results using positive

41   matrix factorization (PMF) further show large seasonal differences in the sources of NACs.

42   Specifically, in summer, NACs were highly influenced by secondary formation and vehicle

43   emissions (~80%), while in winter, biomass burning and coal combustion contributed the most

44   (~75%). Furthermore, the light absorption contributions of NACs to BrC are wavelength

45   dependent and vary greatly by seasons, with maximum contributions at ~330 nm in winter and

46   fall and ~320 nm in summer and spring. The differences in the contribution to light absorption

47   are associated with the higher mass fractions of 4-nitrocatechol (λ_{max}=345 nm) and 4-

48   nitrophenol (λ_{max}=310 nm) in fall and winter, 4-nitrophenol in spring, and 5-nitrosalicylic acid

49   (λ_{max}=315 nm) and 4-nitrophenol in summer. The mean contributions of NACs to BrC light

50   absorption at the wavelength of 365 nm in different seasons are 0.14% (spring), 0.09%

51   (summer), 0.36% (fall) and 0.91% (winter), which are about 6-9 times higher than their mass

52   fractional contributions of carbon in total organic carbon. Our results indicate that the

53   composition and sources of NACs have profound impacts on the BrC light absorption.

54

55   **1 Introduction**

56   Brown carbon (BrC) aerosol has received growing attention over the past years, because

Atmospheric
Chemistry
and Physics
Discussions
Open Access
EGU

57 it can affect the atmospheric radiation balance and air quality through absorption of solar

58 radiation in the near ultraviolet and visible range (Feng et al., 2013; Laskin et al., 2015; Zhang

59 et al., 2017). Nitrated aromatic compounds (NACs) belong to a major group of BrC

60 chromophores. They are ubiquitous in the atmosphere and have been detected in cloud water

61 (Desyaterik et al., 2013), rainwater (Schummer et al., 2009), fog water (Richartz et al., 1990),

62 snow water (Vanni et al., 2001), as well as in gas and particle phases (Cecinato et al., 2005;

63 Zhang et al., 2013; Chow et al., 2015; Al-Naiema and Stone, 2017). Field studies have shown

64 that ~4% of BrC light absorption at 370 nm is contributed by those measured NACs (Zhang et

65 al., 2013; Mohr et al., 2013). In addition, with molecular structures commonly containing nitro

66 (-NO$_2$) and hydroxyl (-OH) functional groups on the aromatic ring, NACs are harmful to human

67 health (Taneda et al., 2004). There is also evidence that NACs affect plant growth and

68 contributed to forest decline (Hinkel et al., 1989; Natangelo et al., 1999). The significant role

69 of NACs in the atmosphere and their adverse effects on ecosystems call for studies to

70 investigate their sources and characteristics.

71   NACs in atmospheric aerosol can be derived from primary emissions, including biomass

72 burning (Wang et al., 2017; Teich et al., 2017; Lin et al., 2018), coal combustion (Olson et al.,

73 2015; Lu et al., 2019a), and vehicle exhausts (Taneda et al., 2004; Inomata et al., 2013; Perrone

74 et al., 2014; Lu et al., 2019b). The emission factors of NACs from biomass burning can be over

75 10 mg kg^{-1} (Wang et al., 2017), which makes them good tracers of biomass burning organic

76 aerosol (BBOA) (Hoffmann et al., 2007; Iinuma et al., 2010). Lu et al. (2019a) determined that

77 the emission factors of fine particulate NACs for residential coal combustion was 0.2-10.1 mg

78 kg^{-1} and the total NAC emission from residential coal burning was nearly 200 Mg in China in

79 2016. NACs from vehicle exhaust also have been detected, with emission factors of up to 26.7

80 μg km^{-1} (Lu et al., 2019b). Secondary formation from various atmospheric reactions is also an

81 important source of NACs. For example, photochemical oxidation of benzene, toluene (Wang

82 et al., 2019), and *m*-cresol (Iinuma et al., 2010) can form certain NACs. NACs can also form

83 in aerosol or cloud water through aqueous-phase reactions (Vione et al., 2001, 2005), for

84 example, photonitration of guaiacol in the aqueous phase (Kitanovski et al., 2014). However,

85 little is known about the importance of primary versus secondary sources for particle-bound

86 NACs because speciation of NACs and quantification of their sources are still very limited so

87 far.

88   Speciation of particle-bound NACs was mostly performed in Europe (Cecinato et al., 2005;

89 Iinuma et al., 2010; Delhomme et al., 2010; Mohr et al., 2013; Kahnt et al., 2013), and still very

90 scarce in Asia (Chow et al., 2015; Wang et al., 2018; Ikemori et al., 2019). In general, the

91 average concentrations of measured NACs vary from less than one to dozens of ng m^{-3} in

92 different seasons and regions. As far as we know, only one study has quantified the sources of

93 NACs with a positive matrix factorization (PMF) receptor model (Wang et al., 2018). Here, we

94 carried out chemical analyses together with light absorption for PM$_{2.5}$ samples collected in

95 Xi'an to: 1) investigate the seasonal variations in the concentration of NACs and contributions

96 of individual species; 2) quantify the sources of NACs in different seasons based on PMF model;

97 and 3) evaluate the optical properties of NACs and their contributions to BrC light absorption.

98 **2 Experiments and methods**

99 **2.1 Aerosol sampling**

100   24 h-integrated PM$_{2.5}$ samples were collected in four seasons from November 2015 to

101 November 2016 (i.e., from 30 November to 31 December 2015 for winter; 19 April to 19 May

102 2016 for spring; 1 to 31 July 2016 for summer; and 9 October to 15 November 2016 for fall) in

103 the campus of the Institute of Earth Environment, Chinese Academy of Sciences (IEECAS,

104 34.22°N, 109.01°E) in Xi'an, China. The sampling site is an urban background site surrounded

105 by residential areas and has no obvious industrial activities. A total of 112 samples were

106 collected on pre-baked (780 °C, 3 h) quartz-fiber filters (20.3 × 25.4 cm, Whatman, QM-A,

107 Clifton, NJ, USA) by a Hi-Vol PM$_{2.5}$ sampler (Tisch, Cleveland, OH) operating at 1.05 m^3 min^{-1}.

108 The filter samples were stored at -20 °C until laboratory analysis.

109 **2.2 Chemical analysis**

110   The concentration of organic carbon (OC) was measured by a Thermal/Optical Carbon

111 Analyzer (DRI, Model 2001, Atmoslytic Inc., Calabasas, CA, USA) with the IMPROVE-A

112 protocol (Chow et al., 2011). Ten NACs and 19 organic markers (see Table S1) were quantified

113 by a gas chromatograph-mass spectrometer (GC-MS) using a well-established approach (e.g.,

Atmospheric
Chemistry
and Physics
Discussions

114   Wang et al., 2006; Al-Naiema and Stone, 2017) and the details are described in Yuan et al.,

115   2020. Baseline separation with symmetrical peak shapes was achieved for the measured NACs

116   (Fig. 1). The linear ranges, instrument detection limit (IDL), instrument quantitation limit (IQL),

117   extraction efficiency, and regression coefficients for the measured NACs are shown in Table

118   S2. The response of calibration curves for the NACs was linear ($R^2 \geq 0.995$) from 10 to 5000

119    $\mu g\ L^{-1}$. The IDL ranged from 2 $\mu g\ L^{-1}$ to 20 $\mu g\ L^{-1}$ except for 5-nitrosalicylic acid (52.6 μg

120   L^{-1}). The IQL ranged from below 10 $\mu g\ L^{-1}$ to 70 $\mu g\ L^{-1}$ except for 5-nitrosalicylic acid (> 100

121    $\mu g\ L^{-1}$). The IDL and IQL are comparable to those in Al-Naiema and Stone (2017) (2.7-14.9

122    $\mu g\ L^{-1}$ for IDL and 8.8-49.5 $\mu g\ L^{-1}$ for IQL) and are sufficient for the quantification of our

123   samples.

124   **2.3 Light absorption of NACs**

125   The UV-Vis spectrophotometer equipped with a Liquid Waveguide Capillary Cell

126   (LWCC-3100, World Precision Instrument, Sarasota, FL, USA) was used to measure the light

127   absorption of methanol-soluble BrC and NAC standards, following the method established by

128   Hecobian et al. (2010). The absorption coefficient (Abs_λ: M m^{-1}) can be obtained from measured

129   absorption data by equation (1):

130    $$Abs_\lambda = (A_\lambda - A_{700}) \frac{V_l}{V_a \times L} \ln(10) \qquad (1)$$

131   where A_{700} is the absorption at 700 nm used to correct for baseline drift, V_l is the volume of

132   methanol used for extracting the filter, V_a is the volume of sampled air, L is 0.94 m for the

133   optical path length used in LWCC, and ln(10) is used to convert the absorption coefficient from

134   log base-10 to natural logarithm.

135   The mass absorption efficiency (MAE: m^2 g^{-1}) of NAC standards in the methanol solvent

136   at wavelength of λ can be calculated as Laskin et al. (2015):

137    $$MAE_{NAC,\lambda} = \frac{A_\lambda - A_{700}}{L \times C} \ln(10) \qquad (2)$$

138   where C (μg mL^{-1}) is the concentration of the NAC standards in the methanol solvent.

139   The light absorption contribution of NACs to BrC at wavelength of λ ($Cont_{NAC/BrC,\lambda}$) can

140   be obtained using equation (3).

141    $$Cont_{NAC/BrC,\lambda} = \frac{MAE_{NAC,\lambda} \times C_{NAC}}{Abs_{BrC,\lambda}} \qquad (3)$$

142   where the C_{NAC} (μg m^{-3}) is the atmospheric concentration of NACs and the $Abs_{BrC,\lambda}$ is the Abs

143   of BrC at wavelength of λ.

2.4 Source apportionment

145   The sources of NACs was resolved by PMF receptor model, which was performed by the

146   multilinear engine (ME-2; Paatero, 1997) through the Source Finder (SoFi) interface encoded

147   in Igor Wavemetrics (Canonaco et al., 2013). The input species include five to ten NACs (as

148   the number of NACs detected varies among seasons) and nineteen additional organic tracer

149   species (see Table S1). These include phthalic acid for secondary formation, picene for coal

150   combustion, hopanes for vehicle emission, fluoranthene, pyrene, chrysene, benzo(a)pyrene,

151   benzo(a)anthracene, benzo(k)fluoranthene, benzo(b)fluoranthene, benzo(ghi)perylene, and

152   indeno[1,2,3-cd]pyrene for combustion emission, and vanillin, vanillic acid, syringyl acetone,

153   and levoglucosan for biomass burning. To separate the source profiles clearly, the contribution

154   of those markers unrelated to a certain source was set to 0 in the respective source profile (see

155   Table S3).

156   To better understand the source origins of the NACs, air mass origins during the sampling

157   period were derived from backward-trajectory analysis. This method was used in trajectory

158   clustering based on the GIS-based software-TrajStat (Wang et al., 2009). The archived

159   meteorological data was obtained from the National Center for Environmental Prediction's

160   Global Data Assimilation System (GDAS). In this study, 72-h backward trajectories terminated

161   at a height of 500 m above ground level were calculated during the study period. The trajectories

162   were calculated every 12 h with stating times at 09:00 and 21:00 local time.

3 Results and discussion

3.1 Seasonal variations of NAC composition

165   The concentrations of NACs show clear seasonal differences, with the highest mean values

166   in winter, followed by fall, spring, and summer (see Fig. 2). The concentration ranges of total

167   NACs were 1.4-3.4 ng m^{-3} (spring), 0.1-3.8 ng m^{-3} (summer), 1.6-44.2 ng m^{-3} (fall), and 20.2-

168   127.1 ng m^{-3} (winter). The average concentrations were 2.1 ± 0.6 ng m^{-3}, 1.1 ± 0.8 ng m^{-3}, 12.9

169   ± 11.6 ng m^{-3} and 56.3 ± 23.2 ng m^{-3}, respectively (see Table S4). Nitrophenols (4-nitrophenol,

170   2-methyl-4-nitrophenol, 3-methyl-4-nitrophenol, 2,6-dimethyl-4-nitrophenol) and

171   nitrocatechols (4-nitrocatechol, 3-methyl-5-nitrocatechol, 4-methyl-5-nitrocatechol) show the

172   highest concentrations in winter and the lowest in summer, while nitrosalicylic acids (3-

173   nitrosalicylic acid, 5-nitrosalicylic acid) show the highest concentrations in winter and the

174   lowest in spring. The average ratios between wintertime and summertime concentrations are a

175   factor of about 40 for nitrophenols, 175 for nitrocatechols, and 21 for nitrosalicylic acids. The

176   large seasonal differences in NAC concentrations might be due to the differences in sources,

177   emission strength and atmospheric formation processes, as discussed below. Table 1

178   summarizes the NAC concentrations measured in this study together with those measured in

179   Europe, the USA and other places in Asia. In general, the NAC concentrations in winter are

180   higher than those in summer, and the observed concentrations of different species are higher in

181   Asia than in Europe and the USA. The only exception is a study in Ljubljana, Slovenia, which

182   shows that in winter nitrocatechol concentrations are higher than those in Asia, likely due to

183   strong biomass burning activities (Kitanovski et al., 2012). The elevated concentrations of

184   NACs in Asia suggest that NACs may have a significant impact on regional climate and air

185   quality in Asia due to its optical and chemical characteristics, as discussed below.

186   Among all measured NACs, 4-nitrophenol, 2-methyl-4-nitrophenol, 3-methyl-4-

187   nitrophenol, 4-nitrocatechol and 5-nitrosalicylic acid were detected in four seasons, 3-methyl-

188   5-nitrocatechol and 4-methyl-5-nitrocatechol in fall and winter, 2,6-dimethyl-4-nitrophenol, 3-

189   nitrosalicylic acid and 4-nitro-1-naphthol only in winter, as shown in Fig. 3a. In general, 4-

190   nitrophenol and 4-nitrocatechol had elevated concentrations in all seasons, which is consistent

191   with other observations (Chow et al., 2015; Ikemori et al., 2019) and might be related to their

192   larger emissions or formation and longer atmospheric lifetime than other NACs (Harrison et al.,

193   2005; Chow et al., 2015; Finewax et al., 2018; Wang et al., 2019; Lu et al., 2019a). For example,

194   Lu et al. (2019a) measured the emission of NACs from coal combustion and founded that the

195   emission factors of 4-nitrocatechol was about 1.5-6 times higher than other NAC. Wang et al.

196   (2019) quantified the concentration of 4-nitrophenol and 4-nitrocatechol formed under high

197   NO_x and anthropogenic VOC conditions, which is about 3-7 times higher than other NAC. The

198   concentration of 2-methyl-4-nitrophenol was higher than that of 3-methyl-4-nitrophenol in all

199 seasons, which is similar to previous studies (Kitanovski et al., 2012; Chow et al., 2015; Teich

200 et al., 2017; Ikemori et al., 2019) and likely due to the efficient formation of 2-methyl-4-

201 nitrophenol from photochemical oxidation of volatile organic compounds (VOCs) in the

202 presence of NO_2 (Lin et al., 2015; Wang et al., 2019). It should be noted that the contribution

203 of 5-nitrosalicylic acid (27%) to total NAC mass in summer is much higher than that in other

204 seasons (4%-13%), suggesting that 5-nitrosalicylic acid is mainly produced by secondary

205 formation, for example, through nitration of salicylic acid (Li et al., 2020), photochemical

206 oxidation of toluene in the presence of NO_x (Jang and Kamens, 2001; Wang et al., 2018).

3.2 Sources of NACs

208   Correlation analysis was conducted among NACs measured in this study (Table S5). The

209 four nitrophenols were positively correlated with each other (r^2 = 0.52-0.98) and the three

210 nitrocatechols were also highly correlated with each other (r^2 = 0.94-0.96), indicating that

211 different nitrophenols and nitrocatechols might have similar sources or origins. Previous studies

212 showed that 4-nitrophenol was mainly from primary emission of biomass burning (Wang et al.,

213 2017), and 3-methyl-5-nitrocatechol and 4-methyl-5-nitrocatechol were identified as secondary

214 products from biomass burning (Iinuma et al., 2010). Positive correlations were also observed

215 between nitrophenols and nitrocatechols (r^2 = 0.59-0.90), suggesting that they were partly of

216 similar sources or formation processes. For example, both nitrophenols and nitrocatechols can

217 be emitted through biomass burning (Wang et al., 2017) and coal combustion (Lu et al., 2019a)

218 and can be formed by photochemical oxidation of VOCs in the presence of NO_2 (Wang et al.,

219 2019). However, for nitrosalicylic acids, the correlation between 3-nitrosalicylic acid and 5-

220 nitrosalicylic acid was weak (r^2 = 0.29). This is because 5-nitrosalicylic acid is mainly from

221 secondary formation by nitration of salicylic acids, while 3-nitrosalicylic acid is mainly from

222 combustion emission (Wang et al., 2017; Li et al., 2020). The correlations between nitrosalicylic

223 acids with nitrophenols (r^2 = 0.01-0.13) and with nitrocatechols (r^2 = 0.04-0.25) were also weak,

224 suggesting that they may have different sources or formation processes. Nitrosalicylic acids

225 were dominated by 5-nitrosalicylic acids, which is mainly from secondary formation

226 (Andreozzi et al., 2006; Wang et al., 2018). On the other hand, nitrophenols and nitrocatechols

227 were dominated by 4-nitrophenol and 4-nitrocatechol, respectively, which are mainly from

228   primary emissions (Wang et al., 2017; Lu et al., 2019a).

229   To identify and quantify the sources of NACs observed in Xi'an, the PMF model was

230   employed and four major factors were resolved with uncertainties < 15%. The factor profiles

231   are shown in Fig. S1. The first factor, vehicle emission, characterized by high levels of hopanes,

232   shows large relative contributions to NACs in spring and summer. Direct traffic emissions of

233   NACs have also been verified in laboratory studies (Tremp et al., 1993; Perrone et al., 2014).

234   The second factor is considered to be coal combustion for residential heating and cooking,

235   which is characterized with the higher loadings of picene, benzo(a)pyrene,

236   benzo(b)fluoranthene, benzo(k)fluoranthene, indeno[1,2,3-cd]pyrene, and

237   benzo(ghi)perylene. This factor accounted for ~40% of the NACs in winter. The emission of

238   NACs from coal combustion for residential usage was reported by Lu et al. (2019a), which

239   showed emission factors of 0.2 to 10.1 mg kg^{-1}. It is worth noting that with the emission control

240   of residential coal burning after 2017, the contribution feature of coal burning to NACs could

241   be different. The third source is identified as secondary formation because of the highest level

242   of phthalic acid and its highest contribution in summer. The formation of secondary NACs is

243   also supported by both field and modeling studies (Harrison et al., 2005; Iinuma et al., 2010;

244   Yuan et al., 2016). The last source factor, with high loadings of levoglucosan, vanillic acid,

245   vanillin and syringyl acetone, was identified as biomass burning, which has higher

246   contributions in fall and winter. The emission of NACs from biomass burning was reported by

247   field studies, and was considered to be an important source of NACs (Mohr et al., 2013; Lin et

248   al., 2016; Teich et al., 2017).

249   The sources contributions for NACs in Xi'an are shown in Fig. 4, which shows obvious

250   seasonal differences. In spring, vehicular emission (41%) was the main contributor to NACs.

251   Secondary formation (26%) and biomass burning (20%) also contributed significantly. In

252   summer, secondary formation had the highest contribution (45%), which was likely due to

253   enhanced photochemical oxidation leading to the formation of NACs. Besides, vehicular

254   emission also contributed significantly (34%) in summer. In fall, biomass burning (45%)

255   contributed the most, while secondary formation (30%) and vehicular emission (23%) also had

256   significant contributions. In winter, coal burning (39%) and biomass burning (36%) were the

257   main contributors, which can be attributed to emissions from residential heating activities. It is

258   worth noting that the absolute concentrations of NACs attributed by vehicle emission (see Table

259   S6) were higher in winter than those in spring and summer, yet these differences of less than

260   20 times are not as significant as the differences (spring and summer vs. winter) for NACs

261   attributed by other primary emissions (> 80 times for coal burning and > 40 for biomass

262   burning). These results indicate that anthropogenic primary sources are the main contributors

263   to NACs in Xi'an. Secondary formation also contributes significantly to NACs, especially in

264   summer. Further comprehensive field studies are necessary for understanding the formation

265   mechanisms of NACs under different atmospheric conditions.

266   **3.3 Backward trajectory analysis of NACs**

267   To reveal the source origins of the NACs, the concentrations of NACs were grouped

268   according to their trajectory clusters that represent different air mass origins, as shown in Fig.

269   5. In general, the air masses from local emissions (Cluster 1 in spring and fall and Cluster 2 in

270   summer and winter), which showed the features of small-scale and short-distance air transport,

271   caused significant increases in NAC concentrations. As for regional transport, the air masses

272   from the neighboring Gansu province across Baoji city before arriving at Xi'an presented

273   higher concentrations of NACs in fall and winter (Cluster 2 and Cluster 3, respectively). In

274   addition, air masses from Xinjiang across Gansu caused increased concentrations of NACs in

275   spring and summer (Cluster 2 and Cluster 1, respectively). A small proportion of air masses

276   from the northwest (Cluster 3 in spring and Cluster 1 in winter), the south (Cluster 3 in summer)

277   and the west (Cluster 3 in fall), which showed long or moderate transport patterns, are related

278   to the lowest concentrations of NACs. This may be due to the long-distance transport or

279   relatively clean air from those regions. In the same season, the source origins of air masses were

280   different between clusters, thus causing the difference in concentrations of NACs. However,

281   the composition of NACs was similar between clusters, which is comparable to the results of

282   Chow et al. (2015).

283   **3.4 Light absorption of NACs**

284   The correlations between NAC concentration and $Abs_{BrC,365}$ for each season are shown in

285   Fig. S2. The correlations are stronger in fall ($r^2 = 0.68$) and winter ($r^2 = 0.63$) compared to those

286   in spring ($r^2 = 0.15$) and summer ($r^2 = 0.40$). These results indicate that NACs are important

287   components of BrC chromophores in fall and winter.

288   Fig. 6 shows the contributions of NACs to BrC light absorption at wavelength from 300

289   to 500 nm ($Abs_{BrC,300-500}$) as well as the carbon mass contributions of NACs to OC. The

290   contributions of NACs to $Abs_{BrC,300-500}$ are wavelength dependent and vary largely in different

291   seasons. High contributions at wavelengths of 350-400 nm were observed in fall and winter,

292   but the contributions in spring and summer were mainly at wavelengths shorter than 350 nm.

293   These results may be due to the high proportion of nitrocatechols in fall and winter (see

294   discussion above), which have strong light absorption at wavelength above 350 nm (see Fig.

295   S3). The seasonal average contributions of NACs to $Abs_{BrC,365}$ were highest in winter (0.91 ±

296   0.30%), followed by fall (0.36 ± 0.22%), spring (0.14 ± 0.04%), and summer (0.09 ± 0.06%)

297   (see Table S4). These contributions were comparable to a previous study where eight NACs

298   were measured (Teich et al., 2017). The contributions of NACs to $Abs_{BrC,365}$ in winter were

299   about 10 times higher compared to those in summer, which could be due to the high emissions

300   of NACs in winter. Alternatively, enhanced atmospheric oxidizing capacity in the summer can

301   lead to enhanced formation of secondary NACs or the degradation/bleaching of certain NACs

302   (Barsotti et al., 2017; Hems and Abbatt, 2018; Wang et al., 2019) which might eventually reduce

303   the contributions in summer. The fractions of NACs to total OC also show obvious seasonal

304   variation, with average contributions higher in winter (0.14 ± 0.05%) and fall (0.05 ± 0.02%)

305   and lower in spring (0.02 ± 0.01%) and summer (0.01 ± 0.01%). The contributions of NACs to

306   BrC light absorption at 365 nm are, however, 6-9 times larger than their carbon mass

307   contributions to total OC. Our results echo previous studies that even small amounts of

308   chromophores can have a non-negligible impact on the optical characteristics of BrC due to

309   their disproportional absorption contributions (Mohr et al., 2013; Zhang et al., 2013; Teich et

310   al., 2017; Xie et al., 2017).

311   The daily contributions of the individual NACs to light absorption of total NACs at

312   wavelength of 300-500 nm are shown in Fig. 7. Similar to the concentration fractions in NACs,

313   nitrocatechols were the main contributors in winter and fall with contributions of 38-65% and

314   18-62%, respectively. On the other hand, nitrophenols dominated in spring and summer with

315   contributions of 61-96% and 27-100%, respectively. As for nitrophenols, 4-nitrophenol was the

316   most important chromophore, followed by 2-methyl-4-nitrophenol, 3-methyl-4-nitrophenol,

317   and 2,6-dimethyl-4-nitrophenol (only observed in winter). As for nitrocatechols, 4-

318   nitrocatechol was the main contributor in four seasons, while 3-methyl-5-nitrocatechol and 4-

319   methyl-5-nitrocatechol also contributed significantly in fall and winter. For nitrosalicylic acids,

320   5-nitrosalicylic acid contributed in all four seasons but contributed the most in summer, while

321   3-nitrosalicylic acid was only observed in winter, which could be attributed to their different

322   sources, as discussed above.

323   The seasonal contributions of individual NACs to total light absorption of NACs at

324   wavelength of 365 nm are shown in Fig. 3b. The relative contribution trends of 4-nitrophenol >

325   4-nitrocatechol > 2-methyl-4-nitrophenol > 5-nitrosalicylic acid > 3-methyl-4-nitrophenol, 4-

326   nitrophenol > 4-nitrocatechol > 5-nitrosalicylic acid > 2-methyl-4-nitrophenol > 3-methyl-4-

327   nitrophenol, 4-nitrocatechol > 4-nitrophenol > 4-methyl-5-nitrocatechol >3-methyl-5-

328   nitrocatechol > 5-nitrosalicylic acid > 2-methyl-4-nitrophenol > 3-methyl-4-nitrophenol, 4-

329   nitrocatechol > 4-methyl-5-nitrocatechol > 4-nitrophenol > 3-methyl-5-nitrocatechol > 2-

330   methyl-4-nitrophenol > 4-nitro-1-naphthol > 5-nitrosalicylic acid > 3-methyl-4-nitrophenol >

331   3-nitrosalicylic acid > 2,6-dimethyl-4-nitrophenol were observed in spring, summer, fall and

332   winter, respectively. These trends were different from their concentration fractions in OC,

333   which may be mainly due to the differences in light absorption ability (see Fig. S3). These

334   results suggest that mere compositional information of NACs might not be directly translated

335   into impacts on optical property, because they have startlingly different absorption properties.

336   **4 Conclusion**

337   In this study, ten individual NAC species were quantified, together with 19 organic

338   markers, in $PM_{2.5}$ in Xi'an, Northwest China. The average concentrations of NACs were 2.1,

339   1.1, 12.9, and 56.3 ng m^{-3} in spring, summer, fall, and winter, respectively. Higher

340   concentrations of NACs in winter than in summer were also observed in previous studies in

341   Asia, Europe and the USA. Four major sources of NACs were identified in Xi'an based on

342   PMF analysis, including vehicle emission, coal combustion, secondary formation and biomass

343   burning. On average, in spring, vehicular emission (41%) was the main contributor of NACs,

344   and secondary formation (26%) and biomass burning (20%) also had relatively large

345   contributions. In summer, secondary formation contributed the most (45%), which was likely

346   due to the enhanced photochemical formation of secondary NACs that outweights photo-

347   degradation/bleaching. Besides, vehicular emission (34%) also had significantly contribution

348   in summer. In fall, biomass burning (45%) contributed the most, and secondary formation (30%)

349   and vehicular emission (23%) also made significant contributions. In winter, coal burning (39%)

350   and biomass burning (36%) contributed the most, which can be attributed to emissions from

351   residential heating activities. Backward trajectory cluster analyses indicate that both regional

352   and local contributions for NACs were significant in Xi'an. Local contributions were 53, 47,

353   66 and 44% in the four seasons, and regional transport was mainly through the northwest

354   transport channel. The light absorption contributions of NACs to BrC were quantified and also

355   showed large seasonal variations. The seasonal average contributions of total NACs to BrC

356   light absorption at wavelength of 365 nm ranged from 0.1% to 0.9%, which were 6-9 times

357   higher than their carbon mass fractions in total OC. Our results suggest that even a small amount

358   of chromophores can have significant impacts on the optical characteristics of BrC and more

359   studies are needed to better understand the seasonal differences in chemical composition and

360   formation processes of NACs and the link with their optical properties.

361

362   *Data availability.* Raw data used in this study are archived at the Institute of Earth Environment,

363   Chinese Academy of Sciences, and are available on request by contacting the corresponding

364   author.

365   *Supplement.* The Supplement related to this article is available online at

366   *Author contributions.* RJH designed the study. Data analysis was done by WY, LY, and RJH.

367   WY, LY and RJH interpreted data, prepared the display items and wrote the manuscript. All

368   authors commented on and discussed the manuscript.

369   *Competing interests.* The authors declare that they have no conflict of interest.

Atmospheric
Chemistry
and Physics
Discussions

370

378

References

Al-Naiema, I. M. and Stone, E. A.: Evaluation of anthropogenic secondary organic aerosol tracers from aromatic hydrocarbons, Atmos. Chem. Phys., 17, 2053–2065, 2017.

Andreozzi, R., Canterino, M., Caprio, V., Di Somma, I., and Sanchirico, R.: Salicylic acid nitration by means of nitric acid/acetic acid system: chemical and kinetic characterization, Org. Process. Res. Dev., 10, 1199–1204, 2006.

Barsotti, F., Bartels-Rausch, T., De Laurentiis, E., Ammann, M., Brigante, M., Mailhot, G., Maurino, V., Minero, C., and Vione, D.: Photochemical formation of nitrite and nitrous acid (HONO) upon irradiation of nitrophenols in aqueous solution and in viscous secondary organic aerosol proxy, Environ. Sci. Technol., 51, 7486–7495, 2017.

Canonaco, F., Crippa, M., Slowik, J. G., Baltensperger, U., and Prévôt, A. S. H.: SoFi, an IGOR-based interface for the efficient use of the generalized multilinear engine (ME-2) for the source apportionment: ME-2 application to aerosol mass spectrometer data, Atmos. Meas. Tech., 6, 3649–3661, 2013.

Cecinato, A., Di Palo, V., Pomata, D., Tomasi Sciano, M. C., and Possanzini, M.: Measurement of phase-distributed nitrophenols in Rome ambient air, Chemosphere, 59, 679–683, doi:10.1016/j.chemosphere.2004.10.045, 2005.

Chow, J. C., Watson, J. G., Robles, J., Wang, X. L., Chen, L. W. A., Trimble, D. L., Kohl, S. D., Tropp, R. J., and Fung, K. K.: Quality assurance and quality control for thermal/optical

398   analysis of aerosol samples for organic and elemental carbon, Anal. Bioanal. Chem., 401,

399   3141−3152, 2011.

400   Chow, K. S., Huang, X. H. H., and Yu, J. Z.: Quantification of nitroaromatic compounds in

401   atmospheric fine particulate matter in Hong Kong over 3 years: field measurement

402   evidence for secondary formation derived from biomass burning emissions, Environ.

403   Chem., 13, 665–673, doi:10.1071/EN15174, 2015.

404   Delhomme, O., Morville, S., and Millet, M.: Seasonal and diurnal variations of atmospheric

405   concentrations of phenols and nitrophenols measured in the Strasbourg area, France,

406   Atmospheric Pollution Research, 16–22, doi:10.5094/APR.2010.003, 2010.

407   Desyaterik, Y., Sun, Y., Shen, X., Lee, T., Wang, X., Wang, T., and Collett, J. L.: Speciation of

408   "brown" carbon in cloud water impacted by agricultural biomass burning in eastern China,

409   J. Geophys. Res.-Atmos., 118, 7389–7399, https://doi.org/10.1002/jgrd.50561, 2013.

410   Feng, Y., Ramanathan, V., and Kotamarthi, V. R.: Brown carbon: a significant atmospheric

411   absorber of solar radiation?, Atmos. Chem. Phys., 13, 8607−8621, 2013.

412   Finewax, Z., de Gouw, J. A., and Ziemann, P. J.: Identification and quantification of 4-

413   nitrocatechol formed from OH and NO_3 radical-initiated reactions of catechol in air in the

414   presence of NOx: implications for secondary organic aerosol formation from biomass

415   burning, Environ. Sci. Technol., 52, 1981–1989, 2018.

416   Harrison, M. A. J., Barra, S., Borghesi, D., Vione, D., Arsene, C., and Olariu, R. I.: Nitrated

417   phenols in the atmosphere: a review, Atmos. Environ., 39, 231−248, 2005.

418   Hecobian, A., Zhang, X., Zheng, M., Frank, N. H., Edgerton, E. S., and Weber, R. J.: Water-

419   soluble organic aerosol material and the light absorption characteristics of aqueous extracts

420   measured over the Southeastern United States, Atmos. Chem. Phys., 10, 5965−5977, 2010.

421   Hems, R. F. and Abbatt, J. P. D.: Aqueous phase photo-oxidation of brown carbon nitrophenols:

422   reaction kinetics, mechanism, and evolution of light absorption, ACS Earth Space Chem.,

423   2, 225-234, 2018.

424   Hinkel, M., Reischl, A., Schramm, K.-W., Trautner, F., Reissinger, M., and Hutzinger, O.:

425   Concentration levels of nitrated phenols in conifer needles, Chemosphere, 18, 2433–2439,

426   1989.

427   Hoffmann, D., Iinuma, Y., and Herrmann, H.: Development of a method for fast analysis of

428   phenolic molecular markers in biomass burning particles using high performance liquid

429   chromatography/atmospheric pressure chemical ionisation mass spectrometry, J.

430   Chromatogr. A, 1143, 168–175, doi:10.1016/j.chroma.2007.01.035, 2007.

431   Iinuma, Y., Böge, O., Gräfe, R., and Herrmann, H.: Methyl-nitrocatechols: atmospheric tracer

432   compounds for biomass burning secondary organic aerosols, Environ. Sci. Technol., 44,

433   8453–8459, doi:10.1021/Es102938a, 2010.

434   Ikemori, F., Nakayama, T., and Hasegawa, H.: Characterization and possible sources of nitrated

435   mono- and di-aromatic hydrocarbons containing hydroxyl and/or carboxyl functional

436   groups in ambient particles in Nagoya, Japan, Atmos. Environ., 211, 91-102, 2019.

437   Inomata, S., Tanimoto, H., Fujitani, Y., Sekimoto, K., Sato, K., Fushimi, A., Yamada, H., Hori,

438   S., Kumazawa, Y., Shimono, A., and Hikida, T.: On-line measurements of gaseous nitro-

439   organic compounds in diesel vehicle exhaust by proton-transfer-reaction mass

440   spectrometry, Atmos. Environ., 73, 195–203, doi:10.1016/j.atmosenv.2013.03.035, 2013.

441   Jang, M. and Kamens, R. M.: Characterization of secondary aerosol from the photooxidation

442   of toluene in the presence of NOx and 1-propene, Environ. Sci. Technol., 35, 3626–3639,

443   2001.

444   Kahnt, A., Behrouzi, S., Vermeylen, R., Safi Shalamzari, M., Vercauteren, J., Roekens, E.,

445   Claeys, M., and Maenhaut, W.: One-year study of nitro-organic compounds and their

446   relation to wood burning in PM_{10} aerosol from a rural site in Belgium, Atmos. Environ.,

447   81, 561–568, https://doi.org/10.1016/j.atmosenv.2013.09.041, 2013.

448   Kitanovski, Z., Grgic, I., Vermeylen, R., Claeys, M., and Maenhaut, W.: Liquid chromatography

449   tandem mass spectrometry method for characterization of monoaromatic nitro-compounds

450   in   atmospheric   particulate   matter,   J.   Chromatogr.   A,   1268,   35–43,

451   doi:10.1016/j.chroma.2012.10.021, 2012.

452   Kitanovski, Z., Cusak, A., Grgic´, I., and Claeys, M.: Chemical characterization of the main

453   products formed through aqueous-phase photonitration of guaiacol, Atmos. Meas. Tech.,

454   7, 2457–2470, https://doi.org/10.5194/amt-7-2457-2014, 2014.

455   Laskin, A., Laskin, J., and Nizkorodov, S. A.: Chemistry of atmospheric brown carbon, Chem.

456   Rev., 115, 4335−4382, 2015.

457   Li, M., Wang, X., Lu, C., Li, R., Zhang, J., Dong, S., Yang, L., Xue, L., Chen, J., and Wang, W.:

458   Nitrated phenols and the phenolic precursors in the atmosphere in urban Jinan, China, Sci.

459   Total Environ., 714, 136760, 2020.

460   Lin, P., Liu, J. M., Shilling, J. E., Kathmann, S. M., Laskin, J., and Laskin, A.: Molecular

461   characterization of brown carbon (BrC) chromophores in secondary organic aerosol

462   generated from photo-oxidation of toluene, Phys. Chem. Chem. Phys., 17, 23312–23325,

463   doi:10.1039/C5CP02563J, 2015.

464   Lin, P., Aiona, P. K., Li, Y., Shiraiwa, M., Laskin, J., Nizkorodov, S. A., and Laskin, A.:

465   Molecular characterization of brown carbon in biomass burning aerosol particles, Environ.

466   Sci. Technol., 50, 11815-11824, 2016.

467   Lin, P., Fleming, L. T., Nizkorodov, S. A., Laskin, J., and Laskin, A.: Comprehensive molecular

468   characterization of atmospheric brown carbon by high resolution mass spectrometry with

469   electrospray and atmospheric pressure photoionization, Anal. Chem., 90, 12493–12502,

470   2018.

471   Lu, C., Wang, X., Li, R., Gu, R., Zhang, Y., Li, W., Gao, R., Chen, B., Xue, L., and Wang, W.:

472   Emissions of fine particulate nitrated phenols from residential coal combustion in China,

473   Atmos. Environ., 203, 10–17, https://doi.org/10.1016/j.atmosenv.2019.01.047, 2019a.

474   Lu, C., Wang, X., Dong, S., Zhang, J., Li, J., Zhao, Y., Liang, Y., Xue, L., Xie, H., Zhang, Q.,

475   and Wang, W.: Emissions of fine particulate nitrated phenols from various on-road

476   vehicles in China, Environmental Research, 179, 108709,

477   https://doi.org/10.1016/j.envres.2019.108709, 2019b.

478   Mohr, C., Lopez-Hilfiker, F. D., Zotter, P., Prévôt, A. S., Xu, L., Ng, N. L., Herndon, S. C.,

479   Williams, L. R., Franklin, J. P., Zahniser, M. S., Worsnop, D. R., Knighton, W. B., Aiken,

480   A. C., Gorkowski, K. J., Dubey, M. K., Allan, J. D., and Thornton, J. A.: Contribution of

481   nitrated phenols to wood burning brown carbon light absorption in Detling, United

482   Kingdom during winter time, Environ. Sci. Technol., 47, 6316–6324,

483   https://doi.org/10.1021/es400683v, 2013.

484   Natangelo, M., Mangiapan, S., Bagnati, R., Benfenati, E., and Fanelli, R.: Increased

485   concentrations of nitrophenols in leaves from a damaged forestal site, Chemosphere, 38,
486   1495–1503, doi:10.1016/S0045-6535(98)00370-1, 1999.

487 Olson, M. R., Garcia, M. V., Robinson, M. A., Van Rooy, P., Dietenberger, M. A., Bergin, M.,
488   and Schauer, J. J.: Investigation of black and brown carbon multiple-wavelength
489   dependent light absorption from biomass and fossil fuel combustion source emissions, J.
490   Geophys. Res., 120, 6682–6697, doi:10.1002/2014JD022970, 2015.

491 Paatero, P.: Least squares formulation of robust non-negative factor analysis, Chemometr. Intell.
492   Lab., 37, 23–35, 1997.

493 Perrone, M. G., Carbone, C., Faedo, D., Ferrero, L., Maggioni, A., Sangiorgi, G., and
494   Bolzacchini, E.: Exhaust emissions of polycyclic aromatic hydrocarbons, n-alkanes and
495   phenols from vehicles coming within different European classes, Atmos. Environ., 82,
496   391–400, 2014.

497 Richartz, H., Reischl, A., Trautner, F., and Hutzinger, O.: Nitrated phenols in fog, Atmos.
498   Environ., 24A, 3067-3071, https://doi.org/10.1016/0960-1686(90)90485-6, 1990.

499 Schummer, C., Groff, C., Chami, J. A., Jaber, F., and Millet, M.: Analysis of phenols and
500   nitrophenols in rainwater collected simultaneously on an urban and rural site in east of
501   France,   Sci.   Total.   Environ.,   407,   5637-5643,
502   https://doi.org/10.1016/j.scitotenv.2009.06.051, 2009.

503 Taneda, S., Mori, Y., Kamata, K., Hayashi, H., Furuta, C., Li, C., Seki, K., Sakushima, A.,
504   Yoshino, S., Yamaki, K., Watanabe, G., Taya, K., and Suzuki, A. K.: Estrogenic and anti-
505   androgenic activity of nitrophenols in diesel exhaust particles (DEP), Biol. Pharm. Bull.,
506   27, 835–837, 2004.

507 Teich, M., van Pinxteren, D., Wang, M., Kecorius, S., Wang, Z., Müller, T., Mocnik, G., and
508   Herrmann, H.: Contributions of nitrated aromatic compounds to the light absorption of
509   water-soluble and particulate brown carbon in different atmospheric environments in
510   Germany and China, Atmos. Chem. Phys., 17, 1653–1672, https://doi.org/10.5194/acp-
511   17-1653-2017, 2017.

512 Tremp, J., Mattrel, P., Fingler, S., and Giger, W.: Phenols and nitrophenols as tropospheric
513   pollutants: emissions from automobile exhausts and phase transfer in the atmosphere,

514   Water Air Soil Poll., 68, 113–123, https://doi.org/10.1007/bf00479396, 1993.

515   Vanni, A., Pellegrino, V., Gamberini, R., and Calabria, A.: An evidence for nitrophenol

516   contamination in Antarctic fresh-water and snow. Simultaneous determination of

517   nitrophenols and nitroarenes at ng/L levels, Int. J. Environ. Anal. Chem., 79, 349-365,

518   http:// doi.org/10.1080/03067310108044394, 2001.

519   Vione, D., Maurino, V., Minero, C., and Pelizzetti, E.: Phenol photonitration upon UV

520   irradiation of nitrite in aqueous solution I: effects of oxygen and 2-propanol, Chemosphere,

521   45, 893–902, https://doi.org/10.1016/s0045-6535(01)00035-2, 2001.

522   Vione, D., Maurino, V., Minero, C., and Pelizzetti, E.: Aqueous atmospheric chemistry:

523   formation of 2,4-dinitrophenol upon nitration of 2-nitrophenol and 4-nitrophenol in

524   solution, Environ. Sci. Technol., 39, 7921–7931, doi:10.1021/es050824m, 2005.

525   Wang, G. H., Kawamura, K., Lee, S., Ho, K. F., and Cao, J. J.: Molecular, seasonal, and spatial

526   distributions of organic aerosols from fourteen Chinese cities, Environ. Sci. Technol., 40,

527   4619-4625, https://doi.org/10.1021/es060291x, 2006.

528   Wang, L. W., Wang, X. F., Gu, R. R., Wang, H., Yao, L., Wen, L., Zhu, F. P., Wang, W. H., Xue,

529   L. K., Yang, L. X., Lu, K. D., Chen, J. M., Wang, T., Zhang, Y. H., and Wang, W. X.:

530   Observations of fine particulate nitrated phenols in four sites in northern China:

531   concentrations, source apportionment, and secondary formation, Atmos. Chem. Phys., 18,

532   4349-4359, 2018.

533   Wang, X., Gu, R., Wang, L., Xu, W., Zhang, Y., Chen, B., Li, W., Xue, L., Chen, J., and Wang,

534   W.: Emissions of fine particulate nitrated phenols from the burning of five common types

535   of biomass, Environ. Pollut., 230, 405–412, https://doi.org/10.1016/j.envpol.2017.06.072,

536   2017.

537   Wang, Y., Hu, M., Wang, Y., Zheng, J., Shang, D., Yang, Y., Liu, Y., Li, X., Tang, R., and Zhu,

538   W.: The formation of nitro-aromatic compounds under high NOx and anthropogenic VOC

539   conditions in urban Beijing, China, Atmos. Chem. Phys., 19, 7649–7665,

540   https://doi.org/10.5194/acp-19-7649-2019, 2019.

541   Wang, Y. Q., Zhang, X. Y., and Draxler, R.: TrajStat: GIS-based software that uses various

542   trajectory statistical analysis methods to identify potential sources from long-term air

Atmospheric
Chemistry
and Physics
Discussions

543   pollution measurement data, Environ. Modell. Softw., 24, 938-939, 2009.

544   Xie, M. J., Chen, X., Hays, M. D., Lewandowski, M., Offenberg, J., Kleindienst, T. E., and

545   Holder, A. L.: Light absorption of secondary organic aerosol: composition and

546   contribution of nitroaromatic compounds, Environ. Sci. Technol., 51, 11607−11616, 2017.

547   Xie, M. J., Chen, X., Holder, A. L., Hays, M. D., Lewandowski, M., Offenberg, J. H.,

548   Kleindienst, T. E., Jaoui, M., and Hannigan, M. P.: Light absorption of organic carbon and

549   its sources at a southeastern U.S. location in summer, Environ. Pollut., 244, 38–46,

550   https://doi.org/10.1016/j.envpol.2018.09.125, 2019.

551   Yuan, B., Liggio, J., Wentzell, J., Li, S.-M., Stark, H., Roberts, J. M., Gilman, J., Lerner, B.,

552   Warneke, C., Li, R., Leithead, A., Osthoff, H. D., Wild, R., Brown, S. S., and de Gouw, J.

553   A.: Secondary formation of nitrated phenols: insights from observations during the Uintah

554   Basin Winter Ozone Study (UBWOS) 2014, Atmos. Chem. Phys., 16, 2139–2153,

555   https://doi.org/10.5194/acp-16-2139-2016, 2016.

556   Yuan, W., Huang, R. J., Yang, L., Guo, J., Chen, Z. Y., Duan, J., Wang, T., Ni, H. Y., Han, Y.

557   M., Li, Y. J., Chen, Q., Chen, Y., Hoffmann, T., and O'Dowd, C.: Characterization of the

558   light-absorbing properties, chromophore composition and sources of brown carbon

559   aerosol in Xi'an, northwestern China, Atmos. Chem. Phys., 20, 5129-5144, 2020.

560   Zhang, X. L., Lin, Y. H., Surratt, J. D., and Weber, R. J.: Sources, composition and absorption

561   angstrom exponent of light-absorbing organic components in aerosol extracts from the Los

562   Angeles Basin, Environ. Sci. Technol., 47, 3685–3693, doi:10.1021/es305047b, 2013.

563   Zhang, Y., Forrister, H., Liu, J., Dibb, J., Anderson, B., Schwarz, J. P., Perring, A. E., Jimenez,

564   J. L., Campuzano-Jost, P., Wang, Y., Nenes, A., and Weber, R. J.: Top-of-atmosphere

565   radiative forcing affected by brown carbon in the upper troposphere, Nat. Geosci., 10,

566   486–489, https://doi.org/10.1038/ngeo2960, 2017.

567

Atmospheric
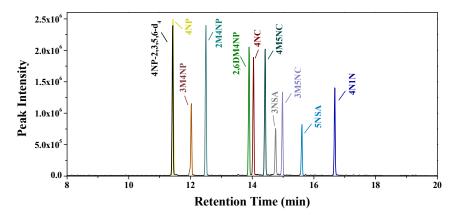Chemistry
and Physics
Discussions

Open Access

EGU

568 **Table 1.** Mean and standard deviation (if applicable) of the measured mass concentrations of

569 individual NAC in Xi'an in comparison to those in other studies.

Locations	Concentrations (ng m^{-3})										Reference
	4NP	2M4NP	3M4NP	2,6DM4NP	4N1N	4NC	3M5NC	4M5NC	3NSA	5NSA	
Europe											
TROPOS, Germany, winter 2014	7.09	3.64	2.60	0.65					1.36	0.94	Teich et al., 2017
	(7.08)	(3.05)	(2.22)	(0.58)					(1.02)	(0.75)	
Melpitz, Germany, summer 2014	0.06	0.04	0.03						0.17	0.09	Teich et al., 2017
	(0.03)	(0.00)	(0.00)						(0.15)	(0.09)	
Melpitz, Germany, winter 2014	4.09	3.64	2.44	0.91					0.66	0.32	Teich et al., 2017
	(3.27)	(3.06)	(2.20)	(0.90)					(0.69)	(0.24)	
Ljubljana, Slovenia, summer 2010	0.15	0.05	<0.03			0.24	0.1	0.06	0.09	0.18	Kitanovski et al., 2012
Ljubljana, Slovenia, winter 2010	1.8	0.75	0.61			75	34	29	1.3	1.4	Kitanovski et al., 2012
Villa Ada park, Rome, spring 2003	17.8		7.8	5.9							Cecinato et al., 2005
	(5.6)		(2.6)	(2.9)							
Waldstein, Germany, summer 2014									0.17	0.23	Teich et al., 2017
									(0.11)	(0.12)	
USA											
Research Triangle Park, USA, summer 2013	0.018	0.005				0.057					Xie et al., 2019
	(0.027)	(0.009)				(0.042)					
Lowa City, USA, fall 2015	0.63	0.08				1.60		1.61		0.14	Al-Naiema and Stone, 2017
	(0.48)	(0.05)				(2.88)		(1.77)		(0.08)	
Asia											
Hong Kong, China, spring 2012	0.36	0.18	0.03	0.01		0.25	0.05	0.05			Chow et al., 2015
Hong Kong, China, summer 2012	0.54	0.3	0.02	0.01		1.48	0.63	0.25			Chow et al., 2015
Hong Kong, China, fall 2012	0.92	0.39	0.04	0.01		2.45	0.94	0.44			Chow et al., 2015
Hong Kong, China, winter 2012	1.13	0.65	0.07	0.01		2.39	1.35	0.53			Chow et al., 2015
Xianghe, China, summer 2013	0.98	0.32	0.09	0.06					1.21	0.88	Teich et al., 2017
	(0.78)	(0.21)	(0.07)	(0.05)					(1.45)	(0.64)	
Wangdu, China, summer 2014	2.63	0.68	0.21	0.06					3.14	1.63	Teich et al., 2017
	(2.66)	(0.78)	(0.35)	(0.09)					(3.05)	(0.78)	
Xi'an, China, spring 2016	1.19	0.24	0.18			0.28				0.15	This study
	(0.36)	(0.08)	(0.05)			(0.18)				(0.15)	
Xi'an, China, summer 2016	0.45	0.10	0.07			0.16				0.29	This study
	(0.28)	(0.10)	(0.06)			(0.11)				(0.41)	
Xi'an, China, fall 2016	3.6	0.73	0.44			3.9	1.23	1.35		1.72	This study
	(2.6)	(0.54)	(0.35)			(4.0)	(1.34)	(1.24)		(2.3)	
Xi'an, China, winter 2015	15.6	4.5	3.4	0.55	1.16	15.5	6.4	6.2	0.84	2.3	This study
	(6.6)	(1.72)	(1.52)	(0.39)	(0.53)	(7.4)	(3.7)	(2.9)	(0.56)	(2.4)	
Nagoya, summer 2013	1.1	0.49	0.17		0.98	0.74		0.081	0.33	0.75	Ikemori et al., 2019
	(0.54)	(0.48)	(0.13)		(1.5)	(0.72)		(0.077)	(0.38)	(0.84)	
Nagoya, Japan, fall 2013	7.0	3.2	1.1		0.76	6.8		1.6	0.27	0.67	Ikemori et al., 2019
	(3.9)	(2.7)	(0.76)		(0.64)	(10.8)		(2.9)	(0.20)	(0.41)	

Figure 1. Selected ion monitoring chromatograms for the nitrated aromatic compound standards (2 ug mL^{-1}). (4NP-2,3,5,6-d$_4$: 4-nitrophenol-2,3,5,6-d$_4$, 4NP: 4-nitrophenol, 3M4NP: 3-methyl-4-nitrophenol, 2M4NP: 2-methyl-4-nitrophenol, 2,6DM4NP: 2,6-dimethyl-4-nitrophenol, 4NC: 4-nitrocatechol, 4M5NC: 4-methyl-5-nitrocatechol, 3NSA: 3-nitrosalicylic acid, 3M5NC: 3-methyl-5-nitrocatechol, 5NSA: 5-nitrosalicylic acid, 4N1N: 4-nitro-1-naphthol).
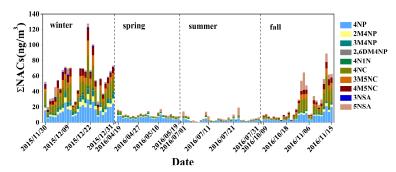
Figure 2. Time series of the concentrations of nitrated aromatic compounds in the aerosol sample (spring and summer × 5, fall ×2). The full names of these compounds are shown in Table S1.
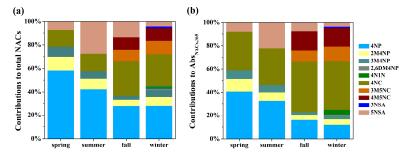
Figure 3. The average contributions of individual nitrated aromatic compounds to (a) the total concentration and (b) the total light absorption at wavelength 365 nm of particulate nitrated aromatic compounds in four seasons. The full names of these compounds are shown in Table S1.
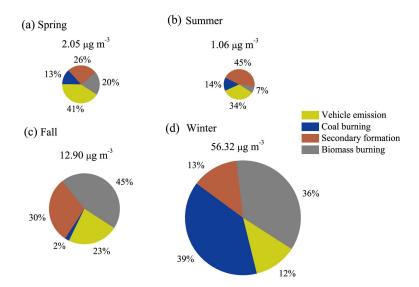
24

(a) Spring

$2.05\ \mu g\ m^{-3}$

26%
13%
20%
41%

(b) Summer

$1.06\ \mu g\ m^{-3}$

45%
14%
7%
34%

Vehicle emission
Coal burning
Secondary formation
Biomass burning

(c) Fall

$12.90\ \mu g\ m^{-3}$

45%
30%
2%
23%

(d) Winter

$56.32\ \mu g\ m^{-3}$

13%
36%
39%
12%

Figure 4. Contributions of source factors to the concentrations of NACs in four seasons.

Figure 5. NACs at each 72-h backward trajectory cluster during (a) spring, (b) summer, (c) fall
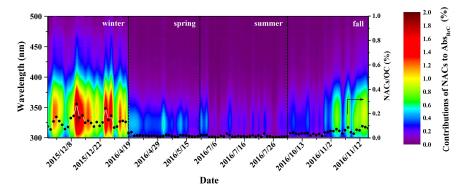and (d) winter. The full names of these compounds are shown in Table S1.

589

Figure 6. Time series of the light absorption contributions of total NACs to Abs of brown carbon over the wavelength from 300 to 500 nm (color scale and left axis), and the ratio of concentration of NACs to organic carbon (dots and right axis).
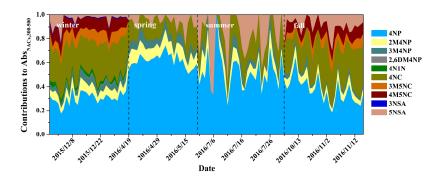
590

591 **Figure 7.** Daily contributions of individual NACs to light absorption of total NACs at

592 wavelength of 300-500 nm. The full names of these compounds are shown in Table S1.